Analysis and Design of an Active Ripple Filter for Dc-Dc Applications

David C. Hamill * and Ong Tiam Toh

Department of Electronic and Electrical Engineering
University of Surrey
Guildford GU2 5XH, United Kingdom

***Abstract* — When low ripple is required from a dc-dc converter, active filters offer an alternative to passive *LC* and coupled inductor filters. A simple experimental active ripple filter is presented, which employs a pair of current transformers as sensors for feedforward and feedback control and two MOSFETs as cancellation current drivers. Measurements demonstrate good ripple attenuation: more than 70dB at 100kHz, and 23dB at 1MHz. The overall efficiency was measured as 95%, but could be improved by attention to the auxiliary supplies to around 98%. The filter is suitable for input and output smoothing in aerospace and other critical applications.**

I. INTRODUCTION

Switched-mode dc-dc converters inherently produce ripple at the switching frequency and its harmonics. This unwanted signal, which appears at both the input and the output, is undesirable for electromagnetic compatibility. Filtering must generally be employed to reduce it to an acceptable level. Passive filters have traditionally been used, but active filters have some attractive features that make them worth investigating.

After a brief survey of filtering techniques, the paper introduces an active filter topology suitable for a spacecraft application. The filter makes use of both feedforward and feedback. Its characteristics are analyzed, the current sensors and driver are discussed, and the system stability is investigated. An experimental circuit is presented, with results demonstrating that good ripple attenuation can be combined with high efficiency.

II. FILTERING TECHNIQUES

A. LC Filters

The filters traditionally used for attenuating ripple are passive low pass *LC* types. For high attenuation they must have low cutoff frequencies — well below the converter's switching frequency — and they can therefore interact dynamically with its control loop. The result can be ringing or even instability. Moreover, the low cutoff frequencies mean that the filter components must be large and heavy: despite the relatively small ripple signals, the series chokes must carry the full through current and the shunt capacitors must withstand the full applied voltage. Although *LC* filters are theoretically 100% efficient, in practice parasitic resistances, especially the winding resistances of chokes, reduce this advantage.

B. Coupled Inductor Filters

When an inductance L is used to smooth a current i, the ripple voltage v appearing across it is non-zero. Since $di/dt = v/L$, the ripple current is also non-zero. But if L is coupled magnetically to a second choke, a voltage can be induced which, under the right conditions, cancels v. Because L sees a zero voltage, di/dt is zero, meaning that i has zero ripple. Thus ripple can be steered away from particular input or output terminals, or confined completely within the converter. This technique is employed to good effect in the isolated Ćuk converter [1], [2]. Very low ripple is achieved at both input and output by coupling the input choke, the output choke and the transformer; all the windings can be combined onto a single core, allowing savings in size and weight.

As with all nulling techniques, this one is not robust against parameter drift. In practice there is a residual ripple current. Furthermore, large coupling capacitors are typically involved. As with conventional *LC* filters, the dynamics of the converter may be adversely affected, and parasitic resistances will cause losses.

C. Active Filters

Active filters offer an alternative approach. In low frequency applications, e.g. at 50–60Hz, switched mode techniques can be employed. But to cope with the frequencies emitted from dc-dc converters, which range from tens of kilohertz to megahertz, non-switched "linear" circuits must be used. Their inherent dissipation makes them less than ideal, but the overall efficiency can nevertheless be acceptable.

* Corresponding author

0-7803-2482-X/95 $4.00

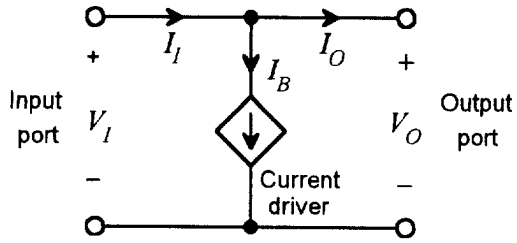

Fig. 1: Dc circuit of the active filter topology.

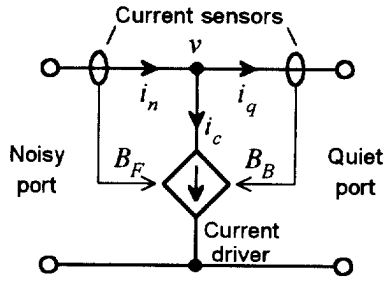

Fig. 2: Ac circuit of the active filter, showing feedforward and feedback paths.

Active ripple filter topologies are of two basic types, which are duals. In *voltage canceling* filters, a voltage is introduced in series with the ripple voltage to cancel it. (This is reminiscent of the coupled inductor technique.) In *current canceling* filters, a cancellation current is injected at a node traversed by the ripple current. An alternative classification, due to LaWhite and Schlecht [3]–[5], describes whether the filter's control circuit senses current or voltage and whether the cancellation signal is applied by means of a current source or a voltage source. Active ripple filters are then classified as voltage or current sensing, voltage or current driving.

III. CHOSEN TOPOLOGY

Ripple filters may equally well be applied to a converter's output or to its input, the case considered here. The application of interest was obtaining low input ripple current for converters drawing about 40W from a spacecraft's dc bus. For various reasons [6] it is often desirable to distribute the power around a spacecraft at a regulated voltage of about 30–50V, transforming it to the required end voltage by dc-dc conversion in each payload module. If standardized converters are employed, their switching frequencies will be similar. There is a risk that the ripple currents might drift into phase; worse, the converters, interacting via the bus impedance, might even lock together. The total ripple current drawn from the bus would then be large, and might interfere with other equipment. In extreme cases it might even shut down the bus regulator.

Because ripple *current* is of interest here, a current canceling filter was chosen. The basic topology comprises the two-port T network shown in Figs. 1 and 2. Considering the dc equivalent circuit (Fig. 1), one port acts as the *input*, being connected to the dc source, while the other acts as the *output*. For ac ripple (Fig. 2), one port is *noisy*, being connected to the switching converter, while the other is *quiet* (ripple free). Note that the association between input or output and quiet or noisy depends on the application. When the filter is placed in the feed to a dc-dc converter, the input is quiet and the output is noisy; but when the filter is placed between a converter and its load, it is the input port that is noisy.

The topology employs two current sensors for improved performance: one for feedforward, the other for feedback. The feedforward works by sensing the ripple current at the noisy port and generating an identical current in the vertical leg of the T, leaving zero ripple current at the quiet port. In theory, feedforward could give perfect ripple cancellation, but the current gain B_F would have to be exactly unity, at all frequencies and amplitudes of interest. This is impossible given the limited bandwidth and nonlinearities of the components involved. Moreover, as with any null method, feedforward is sensitive to parameter drift. Matters could be improved by means of an adaptive null seeking arrangement [7].

The feedback works by sensing the ripple current at the quiet port and driving it towards the desired value of zero. Because this is an error driven system, infinite loop gain would be needed for perfect ripple cancellation. In practice, to avoid instability the loop gain must be restricted at high frequencies, resulting in limited ripple attenuation. Good overall performance can be achieved by a combination of feedforward and feedback, but at the price of an additional current sensor and a little extra circuitry.

IV. ANALYSIS

A. Modeling as Nullors

It is noteworthy that voltage canceling and current canceling filters may be modeled in their ideal forms as nullors, as shown in Fig. 3. A *nullor* [8] is the combination of two ideal circuit elements: the *nullator*, characterized by the branch relation $\{v = 0,\ i = 0\}$, and the *norator*, characterized by $\{v$ = arbitrary, i = arbitrary$\}$. However, further discussion is beyond the scope of this paper.

B. Ripple Attenuation

In an ideal filter, the ripple current i_q at the quiet port would be zero. (See Fig. 2 for symbols.) Thus the whole of

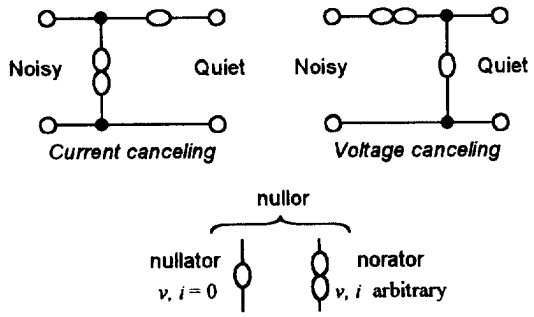

Fig. 3: Representation of active ripple filters as nullors.

the unwanted ripple current i_n at the noisy port would be diverted down the vertical leg of the T, returning to the noisy port. To this end a cancellation current $i_c = i_n$ should be generated in the vertical leg. Inevitably i_c will not match i_n exactly, so the quiet port current i_q will be non-zero. The cancellation current is given by

$$I_c(s) = B_F(s)I_n(s) + B_B(s)I_q(s) \tag{1}$$

where $B_F(s)$ and $B_B(s)$ are the current gains of the feedforward and feedback paths respectively, and $I_c(s)$ is the Laplace transform of $i_c(t)$, etc. By KCL $I_q(s) = I_n(s) - I_c(s)$, so the closed loop current transfer function $B(s)$ can be found as

$$B(s) = \frac{I_q(s)}{I_n(s)} = \frac{1 - B_F(s)}{1 + B_B(s)} \tag{2}$$

For good performance $B(s)$ should be small, so $B_F(s)$ should be as close to unity as possible, while $B_B(s)$ should be as large as possible.

C. Stability

When considered in isolation, the stability of the active filter is determined by the poles of (2), which must lie in the left half of the complex plane.

When the filter is embedded within a system, its stability also depends on the external impedances. If the noisy port is fed by a Thevenin equivalent source of voltage $V_n(s)$ in series with impedance $Z_n(s)$ and the quiet port sees $V_q(s)$ in series with $Z_q(s)$, the voltage $V(s)$ appearing across the vertical leg is given by

$$V(s) = \frac{Z_n(s)V_q(s) + Z_q(s)V_n(s)}{Z_n(s) + Z_q(s)\dfrac{1 - B_F(s)}{1 + B_B(s)}} \tag{3}$$

Thus there will be interaction between the active filter and its neighboring circuitry. For system stability, the poles of (3) must lie in the left half plane. Note that the values of $Z_n(s)$ and $Z_q(s)$ should take into account the impedances of the respective current sensors.

D. Efficiency

In the ideal dc circuit of Fig. 1, $V_I = V_O$. For perfect efficiency, $I_I = I_O$. In practice the vertical leg may need to pass a bias current I_B, depending on the type of current driver employed. The efficiency is then $\eta = I_O/I_I$.

In the design presented below, the current driver consists of a pair of MOSFETs biased to work in Class A. Their drain currents comprise the bias dc I_B with the ripple cancellation current i_c superimposed. To avoid distortion, the total current must never go to zero: $I_B + i_c(t) > 0$ for all t. Now for ideal cancellation $i_c = i_n$, so $I_B \geq I_{n(-pk)}$, where $I_{n(-pk)}$ is the negative peak value of $i_n(t)$; thus the bias current can be chosen. Suppose the limiting case of $I_B = I_{n(-pk)}$ is taken. Since $I_I = I_O + I_B$, and defining a peak ripple factor $r = I_{n(-pk)}/I_O$, the efficiency is

$$\eta = \frac{1}{1 + r} \tag{4}$$

(This expression neglects control circuit and other losses.) The efficiency drops as r increases, suggesting that the active filter is inappropriate for high ripple factors. However, if $r < 0.1$, which should be easily achieved with a little passive filtering, the efficiency $\eta > 90\%$, which is adequate for most purposes.

E. Mass

It is apparent that a practical system design will contain a mixture of active and passive filtering: the active filter will probably be preceded by a passive filter to reduce the ripple to a manageable level. In mass critical applications it is interesting to determine the optimum mix of active and passive filtering. A rough analysis can be carried out as follows.

Other things being equal, it can be argued that the mass m_p of a well designed passive filter rises with its ripple attenuation: $m_p = k_p/B_p$, where k_p is a constant and B_p is the ripple current gain.

The active filter sees a ripple factor r proportional to the ripple current gain B_p of the preceding passive filter. Equation (4) may be manipulated to show that the power lost in the active filter is proportional to r. Assuming that it is dominated by heatsinks, the mass m_a of the active filter is proportional to the heat dissipated. Combining these, $m_a = k_a B_p$.

The total mass is therefore $m = m_p + m_a = k_p/B_p + k_a B_p$. Setting dm/dB_p to zero and solving for B_p, it is found that m has a minimum value $m_{min} = 2\sqrt{k_p k_a}$ when $B_p = \sqrt{k_p/k_a}$. Substituting the latter value into the expressions for m_a and m_p, it is found that they are equal: the total mass is minimized when the passive filter and the active filter weigh the

same. The minimum is quite broad, however, so the balance is not critical: substantial deviations from the optimum will make little difference to the total mass. For instance, B_p can vary over a range of 1.87 : 1 and m will exceed m_{min} by less than 5%.

V. CURRENT SENSORS

It is important that the current sensors accurately reflect the current waveforms they monitor. A variety of different methods of ripple current sensing were considered. A common ground connection between the two ports was thought highly desirable, ruling out a current sensing impedance in the ground line. A floating impedance in the positive line was discarded because the sensing circuit would need excellent common mode rejection up to megahertz frequencies, felt to be impractical. (Nevertheless, a floating inductor feeding a transistor has been used by other workers [3]–[5].)

The final choice was a toroidal current transformer placed in the positive line. The transformer action avoids the need to sense low voltages (or alternatively the need to introduce an undesirably high sensing impedance). Moreover, transformer isolation conveniently allows the secondary circuit to be grounded. Furthermore, if a single primary turn is used, it is easy to put an electrostatic shield between the primary and secondary windings, as shown in Fig. 4. This avoids capacitive coupling of common mode noise voltages into the secondary circuit, an effect which is particularly troublesome at high frequencies.

Although the current transformer is a relatively simple component, it may not be clear how best to design it for this application, where it must cope with a dc bias while providing a wide bandwidth.

A simplified equivalent circuit of the current transformer and its burden resistance is shown in Fig. 4. In practice the "leakage" inductance mainly comprises stray inductance in the primary loop; anyway, it has little effect on the frequency response of V_{out}/I_{in}. It can be shown that if $R << \frac{1}{2}\sqrt{L/C}$, the response has a low frequency corner at $\omega_1 = R/L$ and a high frequency corner at $\omega_2 = 1/RC$. A bandwidth factor may be defined by

$$\frac{\omega_2}{\omega_1} = \frac{L}{R^2 C} \tag{5}$$

For a wideband response, it is clear that L should be large while R and C should be small. However, other considerations need to be taken into account.

- If a large L is achieved by using many secondary turns, then the winding capacitance C will be large, reducing the high frequency response. This suggests that there may be an optimum number of turns that maximizes the bandwidth factor.

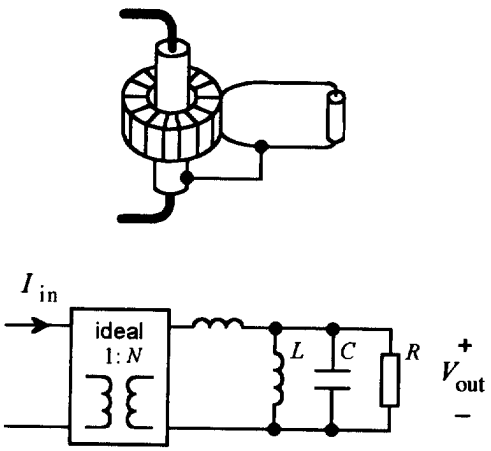

Fig. 4: Current transformer and simplified equivalent circuit.

- Even if a single primary turn is used, the toroidal core must be large enough to avoid saturation: its inside diameter must be greater than $\mu_0\mu_r I_{pk}/\pi B_{sat}$. If a high permeability core material is used to raise L, a larger core will be needed. (The saturation flux density B_{sat} does not vary much among ferrites.)
- A low value of R will give a wide bandwidth, but a smaller output voltage. This will require greater gain from the following amplifier, implying a lower amplifier bandwidth. Therefore there may be an optimum value of R. The situation is complicated by core loss, which is not shown in Fig. 4 but which appears as a frequency dependent resistance in parallel with R.

For empirical investigations, three candidate core materials were tried:

- 3E25 ferrite, a low frequency, medium loss, high permeability manganese–zinc material;
- 4C65 ferrite, a high frequency, low loss, medium permeability nickel–zinc material;
- air — a wideband, zero loss, very low permeability material, with the advantage of perfect linearity. (The current transformer is then better known as a Rogowski coil.)

After some experimentation, the final current transformers were each constructed as 30 turns on a RCC23/7 core of 3E25 ferrite (Philips), feeding a 100Ω burden resistance. A single primary turn was used, with a coaxial copper shield. Careful measurements showed that the transformer introduced phase shifts of less than 10° between 50kHz and 15MHz, with a flat response over this range.

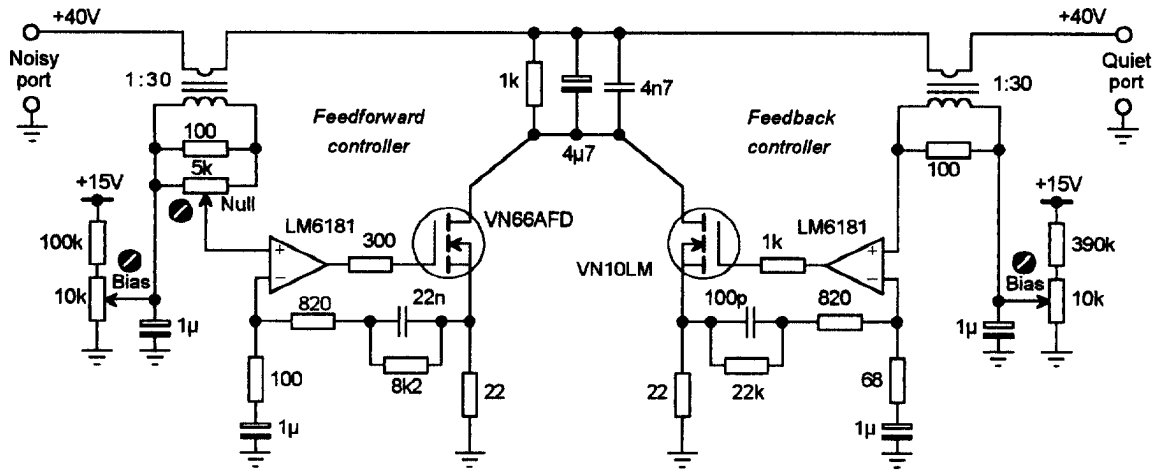

Fig. 5: Circuit diagram of the experimental active ripple filter.

VI. CURRENT DRIVER

The current driver, which injects the cancellation current, is essentially a linear power amplifier. Many different circuits could be used, but a simple Class A MOSFET transconductance amplifier was chosen. The MOSFET requires a substantial dc bias current; although this is somewhat less efficient than other arrangements, the scheme has several advantages:

- It is simple and involves few components.
- Wide bandwidth and low distortion are easily achieved.
- Miller effect is not a problem, as the output drives a low impedance (the positive line).
- No auxiliary supply is needed.

The provision of an auxiliary supply, necessary for most other types of amplifier, is an important practical issue, but one that has generally been overlooked in other published work. Often "magic power supplies" are shown, in which regulated dc appears out of thin air. Such circuits can be misleading, because the cancellation current must circulate around a loop, which usually includes the auxiliary supply. If this is derived from the main dc rail, then significant smoothing must be provided or the object of the active filter will be defeated. It may well be that these additional smoothing components would be better used in a conventional passive ripple filter! The Class A circuit sidesteps the problem, as the MOSFET draws its dc bias from the positive rail. The price is lower efficiency.

VII. CIRCUIT DETAILS

Fig. 5 shows the circuit diagram of the experimental active ripple filter.

A. Selection of Op Amps

Initial tests and calculations revealed that the op amps in the controllers would impose the main high frequency limitation on the filtering. Therefore a wideband op amp was selected, the LM6181 current feedback amplifier (National Semiconductor). This has a unity gain bandwidth of 100MHz, 100 times greater than conventional op amps such as the 741. Gain–bandwidth product is not relevant to current feedback amplifiers: they are designed so that the closed loop bandwidth is largely independent of the closed loop gain. At a gain of ten the 3dB bandwidth of the LM6181 is still about 40MHz. To achieve such performance the feedback resistance should be kept near the recommended value of 820Ω.

Another feature of the LM6181 is its ability to drive high currents into a capacitive load, such as a MOSFET gate, without instability; however, a small resistance should be placed between the op amp's output and the load capacitance to reduce ringing. For stable operation it is essential that the supplies be well decoupled to ground (not shown in Fig. 5). It also helps to keep the input connections as short as possible, and to employ a ground plane, as usual when working at radio frequencies.

B. Feedforward Controller

The first part of the circuit to be commissioned was the feedforward controller. For good ripple cancellation the aim is to keep the current gain $|B_F(j\omega)|$ close to unity, the phase shift $\angle B_F(j\omega)$ small, and to achieve low distortion. The blocks involved are the current transformer, the control amplifier and the current driver.

As described above, the current transformer has a low frequency cutoff due to its magnetizing inductance, and

although this cutoff is well below the switching frequency, it still affects the phase, giving imperfect nulling of the 100kHz fundamental. The 22nF–8.2kΩ network is included in the op amp's local feedback path to compensate. The high frequency rolloffs of the current transformer and the amplifier limit the effectiveness of the feedforward to a few megahertz.

The current driver MOSFET is inherently nonlinear: its V_{GS}–I_D characteristic is approximately parabolic. This factor limited the feedforward nulling of early versions of the circuit, where the amplifier's local feedback was taken directly from its output. By taking the feedback instead from the MOSFET's source terminal, the transistor is included within the loop, effectively linearizing its characteristic. Moreover, the circuit is desensitized to variation in the MOSFET's parameters, an advantage for production designs.

A 300Ω resistor separates the op amp from the gate capacitance; without it, high frequency oscillation occurred. An additional pole is introduced into the local feedback loop. The value of 300Ω was chosen empirically, based on a compromise between stability and high frequency ripple cancellation.

For experimental purposes the MOSFET's bias current is adjustable. The bias is set by observing the voltage waveform at the MOSFET's source and adjusting the potentiometer so that the trough is slightly above zero.

C. *Feedback Controller*

The feedback controller is similar to the feedforward design, except that the aim is to obtain as large a value of $|B_g(j\omega)|$ as possible. As always, the usable high frequency gain is limited by stability considerations. The 100pF–22kΩ–820Ω network in the local feedback path increases the loop gain at low frequencies, resulting in better ripple attenuation below about 2MHz.

D. *Current Drivers*

An earlier version of the circuit employed a single power MOSFET, fed with a composite signal from the feedforward and feedback controllers. Unfortunately, if local feedback is to be taken from the MOSFET's source, a separate transistor is needed for each controller. Because each transistor needs its own bias current, the overall efficiency is worsened. However, the situation is not as bad as it might seem: the bias current is not doubled. This is because the second MOSFET handles only the residual ripple remaining after the feedforward has done its job. The smaller signal permits a lower bias current. A side effect is that a smaller MOSFET can be used, with lower capacitances.

The two drain currents are combined and fed through a 1kΩ resistor, which is included for two reasons: it reduces dissipation in the MOSFETs, and it provides protection against a single-point failure. Without it, a malfunctioning MOSFET could draw excessive current from the positive rail. (There were some spectacular fireworks during development!) However, if unbypassed, the drain voltage would contain a signal component, causing undesirable Miller effect. For this reason the 1kΩ resistor is shunted by capacitance.

Note that power switching MOSFETs were not selected. Low $R_{DS(on)}$ is of no advantage in this application, where the transistors are used in the active region; on the contrary, the associated high gate capacitance would be a drawback.

E. *Auxiliary Power Supplies*

To avoid accusations of "magic" auxiliary power supplies, a simple circuit was devised to power the controllers from the +40V dc rail. It employed a 7815 linear regulator IC to give +15V, and a 7661 voltage converter IC to convert the +15V to −15V. This rather inefficient arrangement worked, but could easily be bettered.

VIII. EXPERIMENTAL RESULTS

To ensure good high frequency performance, the experimental active ripple filter was constructed using rf layout techniques, including a ground plane. As a source of ripple current, a buck converter was set up to switch at 100kHz and draw an input dc of 1A from a 40V dc supply. The converter's input reservoir capacitor was an aluminum electrolytic type with substantial series impedance. With this arrangement the ripple current exported from the converter depends on the reservoir capacitor's impedance and the supply plus line impedance, which are ill defined. To define the Z_n impedance, a small series inductor of 11μH was added at the buck converter's input. The ripple current, shown in the upper trace of Fig. 6, was then approximately triangular and 20mA peak-to-peak.

With the active ripple filter in circuit, the ripple current reduced to that shown in the lower trace of Fig. 6. A spectrum analyzer was used to determine the ripple attenuation at the switching frequency and its harmonics. To ensure that the "with" and "without" results were truly comparable, the active ripple filter was left in place throughout, but the power to the control circuit was disconnected for the "without" readings. The results are given in Table I. Attenuation exceeding 70dB was measured at the 100kHz fundamental, the "with" signal being buried in the instrumentation noise. Attenuation extended up to 5MHz, beyond which some unhelpful amplification occurred.

The system was close to instability at high frequencies,

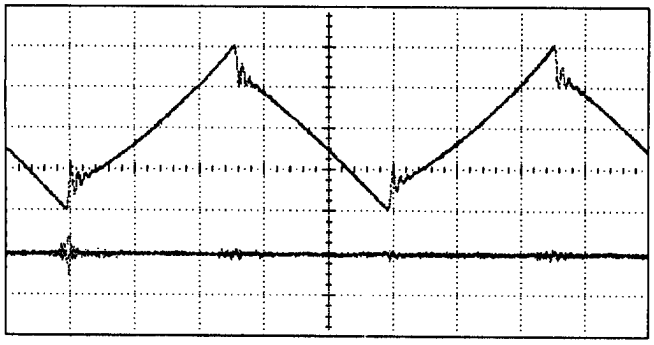

Fig. 6: Measured current waveforms at the active ripple filter's quiet port, $i_g(t)$. Upper trace: active filter disabled; lower trace: active filter enabled. Both traces: 5mA/vertical division, 2μs/horizontal division.

limiting the ripple attenuation attainable. The op amps seem to be responsible, and faster types would be desirable. It might also be advantageous to use different current sensors for feedforward and feedback, so they work over different current ranges.

With a peak ripple factor of 1%, the theoretical efficiency is 99%. The actual efficiency was measured as 95%, and is lower for two reasons: in practice the bias current must exceed the theoretical minimum, and the control electronics must consume some power. The circuit providing the auxiliary ±15V rails was only 38% efficient; if it were improved to say 70% (using a small dc-dc converter fed from the noisy port), the overall efficiency should increase to 98%.

Efficiency could be maximized dynamically through the use of "sliding bias", whereby the MOSFETs' bias current is adjusted automatically to the minimum necessary.

IX. CONCLUSION

The experimental active ripple filter was employed to smooth the input current of a buck dc-dc converter. Ripple at the 100kHz switching frequency was reduced by more than 70dB, with 23dB attenuation at 1MHz. An efficiency of 95% was achieved, but it should be straightforward to modify the auxiliary supplies to bring it to 98%. In applications such as spacecraft, when very low ripple is required, an active ripple filter of this type offers a viable alternative to passive filters.

ACKNOWLEDGMENTS

Thanks are due to K.N. Bateson and M.J. Crawford for helpful discussions on aspects of the active filter design.

TABLE I
MEASURED RIPPLE ATTENUATION

Frequency	Attenuation	
100 kHz	(>70 dB)	*
200 kHz	(>45 dB)	*
300 kHz	47 dB	
400 kHz	(>33 dB)	*
500 kHz	36 dB	
600 kHz	31 dB	
700 kHz	30 dB	
800 kHz	26 dB	
900 kHz	25 dB	
1.0 MHz	23 dB	
1.5 MHz	17 dB	
2.0 MHz	15 dB	
2.5 MHz	14 dB	
3.0 MHz	11 dB	
3.5 MHz	10 dB	
4.0 MHz	6 dB	
4.5 MHz	3 dB	
5.0 MHz	0 dB	

* Signal <10dB above measurement noise floor

REFERENCES

[1] S. Ćuk, Z. Zhang and L.A. Kajouke, "Low profile, 50W/in³, 500kHz integrated-magnetics PWM Ćuk converter", *High Freq. Power Conv. Conf.*, San Diego CA, May 1988, pp. 442–463

[2] D.C. Hamill, "Lumped equivalent circuits of magnetic components: the gyrator–capacitor approach", *IEEE Trans. on Power Electronics*, vol. 8, no. 2, pp. 97–103, Apr. 1993

[3] L.E. LaWhite and M.F. Schlecht, "Active filters for 1-MHz power circuits with strict input/output ripple requirements", *IEEE Trans. on Power Electronics*, vol. 2, no. 4, pp. 282–290, 1987

[4] L.E. LaWhite and M.F. Schlecht, "Design of active ripple filters for power circuits operating in the 1–10 MHz range", *IEEE Trans. on Power Electronics*, vol. 3, no. 3, pp. 310–317, 1988

[5] T. Farkas and M.F. Schlecht, "Viability of active EMI filters for utility applications", *IEEE Trans. on Power Electronics*, vol. 9, no. 3, pp. 328–337, May 1994

[6] D. O'Sullivan, "Space power electronics — design drivers", *ESA Journal*, vol. 18, pp. 1–23, 1994

[7] P. Midya and P.T. Krein, "Feedforward active filter for output ripple cancellation", *International Journal of Electronics*, vol. 77, no. 5, pp. 805–818, Nov. 1994

[8] J.A. Svoboda, "Using nullors to analyse linear networks", *J. Circuit Theory & Appl.*, vol. 14, pp. 169–180, 1986